1981-09

Verification of the bulk method for calculating overwater optical turbulence

Davidson, K.L.

Verification of the bulk method for calculating overwater optical turbulence

K. L. Davidson, G. E. Schacher, C. W. Fairall, and A. K. Goroch

A two-week overwater experiment has been performed to verify the bulk aerodynamic method for calculating the index of refraction structure function parameter, C_N^2. Meteorological data were obtained on shipboard adjacent to a 13-km optical path over Monterey Bay. Model C_N^2 and measured C_N^2 values agree to within 33% on the average when there is spatial homogeneity. During periods of strong sea-surface temperature gradients, disagreements by a factor of 10 are common.

I. Introduction

For several years we have undertaken detailed experimental studies of the properties of the marine atmospheric surface layer. One aspect of these studies has been the structure of small scale turbulence of wind, temperature, and water vapor and the resulting fluctuations of the optical index of refraction. The goal has been to verify the aerodynamic method[1] for calculating optical properties for the overwater regime. Standard mean meteorological parameters of wind speed, relative humidity, air temperature, and sea-surface temperature are the only inputs needed to utilize the methods.

To assess optical turbulence with readily available shipboard meteorological measurements, it is necessary to relate the propagation properties (scintillation) to the turbulence variance statistics and then relate turbulence to the bulk parameters. The theoretical understandings of these relations are good.[2] The relations have been verified experimentally for the overland regime, and relating turbulence statistics to mean parameters has been verified for the overwater regime. However, for the overwater regime, observational verification is based mainly on small scale turbulence measurements rather than on optical results. Of particular concern is the role of humidity fluctuations, which are not a factor in the well-verified overland regime.[3] The scaling of the humidity effect is not as well documented as that for temperature.[4,5] The purpose of this study was to evaluate a bulk model for assessing optical turbulence properties of the marine atmospheric surface layer. The evaluation is based on simultaneous optical and meteorological measurements over the ocean's surface.

The results reported here pertain to bulk methods developed at the Naval Postgraduate School (NPS) from 1973 to 1977. These were first used to evaluate the results of the CEWCOM-78 experiment.[6] Subsequently, considerable effort has gone into determining and verifying the correct scaling for the temperature and humidity structure function parameters, C_T^2 (Ref. 1) and C_Q^2,[5] the humidity-temperature covariance structure function parameter, C_{TQ},[5] and the rate of dissipation of turbulent kinetic energy ϵ.[7] The results have made possible the completion of the formulation of the model for the optical index of refraction structure function C_N^2. In 1979 a workshop was hosted by the Naval Environmental Prediction Research Facility (NEPRF) to recommend improvements to the basic model.[8] In this paper we present results from both the basic and workshop model for comparison purposes.

To test the bulk model with optical data, investigators from NPS and the NEPRF planned a series of coincident optical and meteorological measurements in Monterey Bay from 28 April to 9 May 1980. The Environmental Physics Group of NPS in cooperation with the NPS Optical Propagation Group and Airborne Research Associates (ARA) performed the measurements. The purpose of this effort was to verify overwater optical propagation models which have been de-

A. K. Goroch is with U.S. Naval Environmental Prediction Research Facility, Monterey, California 93940; C. W. Fairall is with BDM Corporation, Monterey, California 93940; and the other authors are with Naval Postgraduate School, Environmental Physics Group, Monterey, California 93940.

Received 10 March 1981.

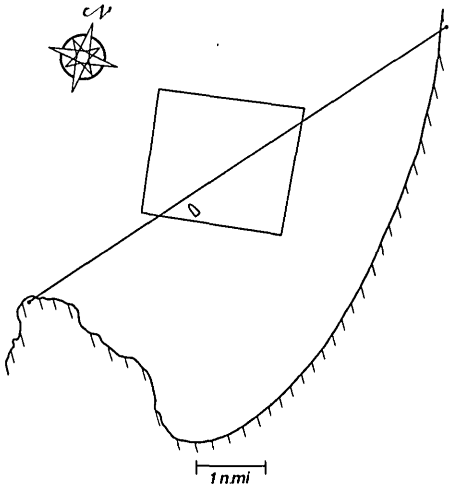

Fig. 1. Experimentation area.

veloped to assess aerosol extinction and small scale turbulence. Verification of the C_N^2 model only is reported here. Evaluation of the boundary layer aerosol model is continuing and will be reported later.

A full range of meteorological measurements, including both mean and fluctuating parameters, was made on the R/VACANIA and the ARA aircraft. Model evaluation reported here uses the shipboard data. Optical measurements were made on a 13-km overwater range[9] and will be described in a separate publication. The ship was frequently stationed on the optical path for direct comparison with the optical measurements over an eight-day period. This occurred at various times of day in order to experience as wide a range of conditions as possible.

II. Experimental Configuration

During periods of simultaneous optical and meteorological measurements, the R/VACANIA was anchored immediately adjacent to the optical path near its midpoint or was sailing within a limited area that straddled the path, as shown in Fig. 1. This section will describe and summarize only the meteorological measurements. A more complete description of the experimental equipment and the various signal processing techniques is available elsewhere.[10]

The ship was equipped with airflow sensors at two levels, 7 and 20 m above the mean sea level. At both levels mean wind speed, temperature, dewpoint, and wind speed fluctuation were measured. Wind direction was measured at the upper level, temperature and humidity fluctuations at the lower level. Sea-surface temperature was determined by both an IR radiometer and a floating sensor which averaged over the upper 30 cm of the water. The IR thermometer was mounted on a railing on an upper deck of the ship and was inclined at an angle of 45°. This inclination angle kept it from viewing the wake of the ship and is near the Brewster angle so that reflected radiation was minimized.

Temperature and wind speed fluctuations were measured with resistance wires, humidity fluctuations were measured with a Lyman-α type sensor. The primary configuration for temperature fluctuations was two wires placed 30 cm apart. Temperature–humidity covariance measurements were made with a single resistance wire placed immediately adjacent to the active volume of the Lyman-α.

All data obtained on the ship were for half-hour averages and hence represent properties of the air passing its location during a one-half hour period. The optical measurements represented properties integrated over the 13-km path length. We are thus comparing a time average and a space average. If there is horizontal homogeneity along the mean wind direction, the time average taken at the ship is equivalent to a space average along the mean wind. The two averages obtained by the optical technique and by the meteorological measurements are not exactly equivalent because the former are normal to the mean wind direction. The precise effects of this in comparisons of optical and meteorological results cannot be determined without detailed knowledge of the local airflow and temperature patterns. This point has been discussed by Wyngaard and Clifford,[11] who indicated that time average and space average are equivalent when the line measurement (optical) is averaged over a time interval of ~1% that of the point measurement. The optical measurement in this case was averaged over 40 sec. This is considered sufficient time to relate directly to the aerodynamic turbulence value, which is considered to be about a 20-min averaging time. This point is under continuing investigation.

The general conditions during all periods were low to moderate winds ($U < 5$ m/sec) and neutral to unstable stratification. The role of the near surface gradients and general stratification is important because the empirical scaling expressions are better established for unstable conditions and when the temperature–humidity covariance is positive.[12]

III. Theory and Bulk Model Consideration

The optical refractive-index structure function parameter is related to the structure functions by

$$C_N^2 = (79 \times 10^{-6}\,P/T^2)^2(C_T^2 + 0.113\,C_{TQ} + 3.1 \times 10^{-3}\,C_Q^2, \quad (1)$$

where P is the pressure in millibars and T is the absolute temperature. The structure function parameter for a quantity y is given by

$$C_y^2 = [y(x) - y(x+d)]^2/d^{2/3}, \quad (2)$$

where $y(x)$ and $y(x + d)$ are values of the quantity at two points separated by a distance d along a line perpendicular to the mean wind direction.

The bulk method or model uses the differences in the values of mean parameters between the sea surface and a reference height to estimate heat, moisture, and momentum flux, which ultimately determine C_N^2. Values of wind, temperature, and some measure of water vapor

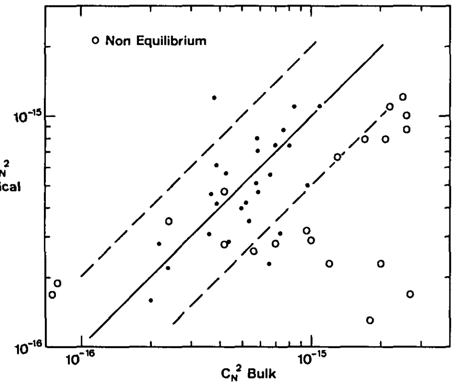

Fig. 2. C_N^2-optics vs C_N^2-bulk model. Open circles are nonequilibrium conditions, solid line is perfect agreement, and dashed lines are a factor of 2 disagreement.

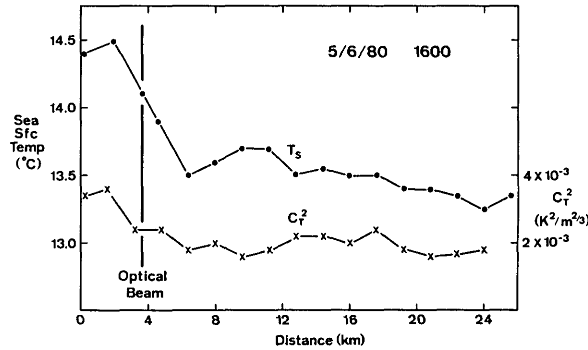

Fig. 3. Aircraft measured IR sea-surface temperature and C_T^2 vs distance from shore. Optical path location is shown by vertical dark line.

content are made at a reference height Z. The sea-surface temperature is measured, the wind is assumed to be zero, and the relative humidity is assumed to be 100% at the surface.

These parameters are used to calculate the quantities needed to determine the appropriate structure functions. The model and the workshop improvements are described fully in the Appendix.

IV. Results

We have compared C_N^2 values obtained from both the bulk model and from the turbulence measurements with optically measured values. For these comparisons we assume that the optical values are correct so the meteorologically derived values are judged by how well they compare to the optical. We note that these comparisons are only being made with data obtained under unstable conditions.

Comparisons of C_N^2 values calculated from the basic bulk model with those measured optically are shown in Fig. 2. The solid points are for cases where the surface layer is in equilibrium, and the open circles are for nonequilibrium conditions, which will be explained below. The solid line indicates perfect agreement, and the two dashed lines correspond to factor of 2 differences, above and below. For all but three of the eighteen cases where the surface layer was in equilibrium the agreement is within a factor of 2. The mean percent error for all equilibrium values is 33%. This is very good agreement for comparisons with these types of data.

We found that, at times, there was a horizontal surface temperature gradient in Monterey Bay in the vicinity of the optical beam. The change was from colder to warmer as the shore was approached. As implied above, the horizontal temperature gradient was not always present, and the actual nature and frequency of occurrence have not been completely determined. Figure 3 shows a plot of sea-surface temperature vs position as measured from the ARA aircraft during one flight using an IR thermometer. The aircraft flew a course perpendicular to the optical path from 2 km offshore to 25 km out to sea. The location of the optical path is shown in the figure by a heavy vertical line. The water temperature is seen to increase gradually (but not monotonically) by a few tenths of a degree up to ~8 km from shore then increases by one degree over a distance of 4 km. The optical path was in the middle of the rapid change region on the day the profile shown was determined.

It was fairly easy to determine from shipboard measurements the days when the sea-surface temperature gradient existed. The shipboard operation required moving in and out of the bay frequently, so it was possible to compare bay temperatures to those farther out to sea. On several days the surface temperature at the optical path was ~1° higher than those seaward and upwind. We assume that the surface layer may not be in equilibrium at the ship site when the large temperature gradient occurs nearby and have indicated data from such days by open circles in Fig. 2. Also during such times the optical path may also be inhomogeneous.

Calculated C_N^2 values for inhomogeneous conditions average a factor of 4 times the optically measured values, which is completely different from the results for the equilibrium cases. The failure of the model for nonequilibrium is easily understood: an elevated sea-surface temperature was measured at the ship which resulted in a large calculated C_N^2 due to the large air–sea temperature difference. How much error in the bulk calculation will result depends on the distance over which the surface layer has adjusted to the new surface temperature. Supporting evidence for this effect was obtained by the aircraft measurements of C_T^2 (Fig. 3). From 25 km at sea to the region of the optical beam C_T^2 was fairly constant then rose about 70% closer to shore. The thermal turbulence did not respond instantly to the temperature change, as suggested by the bulk model calculations.

We do not show the comparison of the turbulence determined C_N^2 values with the optical values but merely state the results. It is well known that salt buildup on the microthermal detectors cause erroneous measurements.[13] To obtain valid data frequent washing of the sensors and signal monitoring are needed. This is very time consuming in a field program and can only be imperfectly done. It was done for this cruise in an attempt to produce as accurate a data set as possible. We have not been able to achieve results as good as with the bulk technique.

If the thermal turbulence measurements could be made correctly, this method should be superior to the bulk model calculation since the small scale turbulence which is primarily responsible for optical scintillation would be measured directly.

The model improvements suggested by the workshop have been applied to these calculations. We do not show the results separately because they made no significant change in the results from the basic model. This is not to say that for conditions further from neutral the improvements would not be significant. The verifications reported here are for a limited range of conditions.

V. Conclusions

These results show the following:

(1) Bulk method estimation of C_N^2 can be expected to be correct to within 50% for situations where horizontal homogeneity exists on a scale of the order of 10 km upwind.

(2) For inhomogeneous conditions, calculated C_N^2 values can be considerably in error, the error depending on the magnitude of local gradients.

(3) The bulk method is superior to direct measurements of small scale turbulence for predicting C_N^2.

In the open ocean, sea-surface temperatures are more uniform than in the near coastal region, and the occurrence of gradients sufficient to affect bulk method calculations should be uncommon.

We have performed bulk model calculations using IR measured sea-surface temperatures. No correction was applied for reflected radiation from the sea surface or constant offset. There was very little agreement between the calculated and optically measured values. Correcting for reflection would improve the comparison, and this is being undertaken, but we expect the result will still not be as good as using the bulk water temperature measurement. In any event, using the bulk measured temperature with no correction applied for surface-film temperature effects has produced very good results, which is somewhat surprising. Common belief is that the film temperature is needed as the boundary condition at the air–sea boundary. We have shown that, for our bulk model, the bulk water temperature is a good boundary temperature.

The authors wish to thank E. C. Crittenden, E. A. Milne, A. W. Cooper, G. W. Rodeback, and S. H. Kalmbach for making the results of their optical propagation measurements available to us. This work was supported by the Navy High Energy Laser Program Office and the Navy EO/MET Program.

Appendix

C_X^2 can be related to the measured meteorological quantities through Monin-Obukhov surface layer similarity parameters:[2,14]

$$C_T^2 = T_*{}^2 Z^{-2/3} f(\zeta), \tag{A1a}$$

$$C_Q^2 = Q_*{}^2 Z^{-2/3} A f(\zeta), \tag{A1b}$$

where T_* is the potential temperature scaling parameter, Q_* is the water vapor density scaling parameter (gm/m^3), Z is the height above the surface, $\zeta = Z/L$ is the similarity (dimensionless) height parameter, and $f(\zeta)$ is the empirical function found by Wyngaard *et al.* The quantity A is a constant approximately equal to 0.6.[4,15,16] The cospectral function is given by

$$C_{TQ} = r_{TQ} T_* Q_* Z^{-2/3} A^{1/2} f(\zeta), \tag{A2}$$

where r_{TQ} is the temperature–humidity correlation parameter equal to 0.8 under unstable conditions. The value of r_{TQ} for stable conditions is not well known in the surface layer. Note that Q_* in (gm/m^3) and q_* in (gm/kg) are related by $Q_* = 1.3q_*$ at the surface. The water vapor mixing ratio scaling parameter is q_*. The Monin-Obukhov length scale L is defined by

$$L = (T/kg) U_*{}^2 (T_* + 6.1 \times 10^{-4}\, Tq_*)^{-1}, \tag{A3}$$

where k is von Karman's constant (0.35), g is the acceleration of gravity, and U_* is the friction velocity.

The problem of predicting C_N^2 is now reduced to finding values for q_*, T_*, and ζ (or L). The bulk method is based on obtaining values of temperature, relative humidity, and wind speed at the sea surface and at some reference height Z. The difference between the surface value and the value at height Z can be related to the scaling parameter through the profile equations[17]

$$U_* = kU[\ln(Z/Z_0) - \psi_U(\zeta)]^{-1}, \tag{A4a}$$

$$T_* = (T - T_S)\alpha_T k[\ln(Z/Z_{0T}) - \Psi_T(\zeta)]^{-1}, \tag{A4b}$$

$$q_* = (q - q_S)\alpha_T k[\ln(Z/Z_{0T}) - \Psi_T(\zeta)]^{-1}, \tag{A4c}$$

where α_T is the ratio of heat transfer to momentum transfer for $\zeta = 0$. Businger *et al.*[18] found $\alpha_T = 1.35$; others have found different values. The quantities Z_0 and Z_{0T} are the roughness lengths for velocity and temperature profiles. Note that these equations can be written in the standard drag coefficient form

$$U_* = c_D^{1/2} U, \tag{A5a}$$

$$T_* = c_T^{1/2}(T - T_S), \tag{A5b}$$

$$q_* = c_T^{1/2}(q - q_S). \tag{A5c}$$

In Eqs. (A4) and (A5), we have assumed that the water vapor dependences q can be treated with the same coefficients as the temperature (Z_{0T}, c_T, α_T).

The stability dependence of the drag coefficients can be obtained from Eqs. (A4) and (A5):

$$c_D^{1/2} = (k/\ln Z/Z_0)[1 - (\ln Z/Z_0)^{-1}\Psi_U(\zeta)]^{-1}. \tag{A6}$$

We can define the neutral stability drag coefficients in terms of the roughness lengths as

$$c_{DN}^{1/2} = k(\ln Z/Z_0)^{-1}, \tag{A7a}$$

$$c_{TN}^{1/2} = \alpha_T k(\ln Z/Z_{0T})^{-1}. \tag{A7b}$$

Note that given the drag coefficient at height Z, one can calculate the roughness length

$$Z_0 = Z \exp(-k/c_{DN}^{1/2}), \tag{A8a}$$

$$Z_{0T} = Z \exp(-\alpha_T k/c_{TN}^{1/2}). \tag{A8b}$$

We are now able to calculate the atmospheric stability at height Z, $\zeta = Z/L$, using Eqs. (A3), (A4), and (A7),

$$\zeta = \zeta_0 \frac{[1 - (\ln Z/Z_0)^{-1}\Psi_U(\zeta)]^2}{1 - (\ln Z/Z_{0T})^{-1}\Psi_T(\zeta)}, \tag{A9}$$

when

$$\zeta_0 = (kgZ/T)(c_{TN}^{1/2}/c_{DN})(\Delta T + 6.1 \times 10^{-4} T\Delta q)U^{-2}. \tag{A10}$$

1. Empirical Constants and Quantities

We have been using a value of von Karman's constant $k = 0.35$ based on the original Businger *et al.* work. Recently, Garratt[19] published a survey which implies $k = 0.41$. Businger *et al.*[17] found $\alpha_T = 1.35$; however, if one uses $k = 0.41$, a value of $\alpha_T = 1.15$ would maintain a constant $\alpha_T k$.

A typical value of c_{DN} at $Z = 10$ m is 1.3×10^{-3}, which yields $Z_0 = 6 \times 10^{-4}$ m. In Kondo[20] and Garratt[19] both equations are for wind speed dependence of the Z = 10-m drag coefficient. Kondo's formulas are used in our model formulation and are given in Table I.

Table I. Wind Speed vs c_{DN} at 10 m from Kondo[20]

U (msec^{-1})	$c_{DN} \times 10^3$
0.3–2.2	$1.08 \times U^{-0.15}$
2.2–5.0	$0.77 + 0.086 \times U$
5.0–8.0	$0.87 + 0.067 \times U$
8.0–25.0	$1.2 + 0.025 \times U$

The temperature drag coefficient has been measured by several groups (see Davidson *et al.*[1] for a summary), but we feel a best estimate is $c_{TN} = 1.3 \times 10^{-3}$ at $Z = 10$ m. Assuming $\alpha_T = 1.35$, we obtain $Z_{0T} = 2.0 \times 10^{-5}$ m. For our bulk model, we assume that Z_{0T} is independent of wind speed and that the wind speed dependence of Z_0 can be obtained from Kondo's c_{DN} using Eq. (A6) with $Z = 10$ m.

2. Iteration Procedure

(1) Input data are sea surface temperature T_S, air temperature T, relative humidity or dew point H or T_D, and wind speed U. The last three are measured at a reference height Z. From T and H (or T_D) calculate q. From T_S calculate q_S assuming that H = 100% at the surface.

(2) From U, calculate c_{DN} (Kondo) for $Z = 10$ m. From c_{DN}, $Z = 10$, calculate Z_0 [Eq. (A7a)]. Let $Z_{0T} = 2.0 \times 10^{-5}$. Let $c_{TN} = 1.3 \times 10^{-3}$ if $Z = 10$ m. If $Z \neq 10$ m, use Eqs. (A5a) and (A5b) to calculate the drag coefficients.

(3) From $\Delta T = T - T_S$ (potential temperature), $\Delta q = q - q_S$, $U = U$, calculate ζ_0 [Eq. (A10)].

(4) Solve Eq. (A9) iteratively to obtain ζ from ζ_0. Note that $L = Z/\zeta$.

(5) From T_*, $Q_* = 1.3\, q_*$, and Z/L calculate C_T^2, C_Q^2, and C_{TQ} at any height using Eqs. (A1) and (A2). Finally calculate C_N^2 from Eq. (1).

3. Stability Correction Functions

Velocity profile:

$$\Psi_U(\zeta < 0) = 2\ln[(1 + x)/2] + \ln[(1 + x^2)/2] - 2\tan^{-1}(x) + \pi/2,$$

$$x = (1 - 15\zeta)^{1/4},$$

$$\Psi_U(\zeta > 0) = -4.7\zeta.$$

Temperature profile:

$$\Psi_T(\zeta < 0) = 2\ln[(1 + x)/2],$$

$$x = (1 - 9\zeta)^{1/2},$$

$$\Psi_T(\zeta > 0) = -6.5\zeta.$$

4. Workshop Improvements

It was recommended that the bulk water temperature be modified to take the surface-film temperature difference into account. The correction is

$$T_s = T_s(\text{bulk}) - 0.025T_a - 0.1 \qquad (U < 6 \text{ msec}^{-1})$$

$$T_s = T_s(\text{bulk}) - 0.1T_a - 0.8 + U(0.117 + 0.0125T_a) \qquad (U > 6 \text{ msec}^{-1}).$$

Here T_a is the measured air temperature, not potential temperature.

The stability parameter Z/L is calculated from

$$\frac{Z}{L} = \frac{gkZT_*}{(T_a + 273.16)\, U_*^2}\left(1 + \frac{0.07}{B_0}\right).$$

B_0 is the Bowen ratio

$$B_0 = \frac{C_p}{L_H}\frac{T_*}{Q_*},$$

C_p is the specific heat of air, and L_H the heat of evaporation of water.

References

1. K. L. Davidson, T. M. Houlihan, C. W. Fairall, and G. E. Schacher, Boundary Layer Meteorol. **15**, 507 (1978).
2. J. C. Wyngaard, Y. Izumi, and S. A. Collins, Jr., J. Opt. Soc. Am. **61**, 1646 (1971).
3. K. F. Schmitt, C. A. Friehe, and C. H. Gibson, J. Phys. Oceangr. **8**, 115 (1978).
4. M. L. Wesely, J. Geophys. Res. **84**, 3696 (1979).
5. C. W. Fairall, G. E. Schacher, and K. L. Davidson, Boundary Layer Meteorol. **19**, 81 (1980).
6. C. W. Fairall, G. E. Schacher, K. L. Davidson, and T. M. Houlihan, "Atmospheric Marine Boundary Layer Measurements in the Vicinity of San Nicholas Island," NPS report NPS61-78-007 (Sept. 1978).
7. G. E. Schacher, K. L. Davidson, and C. W. Fairall, Boundary Layer Meteorol. **20**, 321 (1981).
8. S. D. Burk, A. Goroch, A. Weinstein, and H. Panofsky, "Modeling the Refractive Index Structure in the Marine Planetary Boundary Layer," NEPRF Technical Report TR78-03 (1979).
9. E. C. Crittenden, E. A. Milne, A. W. Cooper, G. W. Rodeback, and S. H. Kalmbach, "Overwater Optical Scintillation Measurements during MAGAT-8," NPS Report NPS-61-80-018 (1980).
10. G. E. Schacher, D. E. Spiel, C. W. Fairall, and K. L. Davidson, "Details of NPS Shipboard and Aircraft Meteorological Measurements Systems," NPS Report NPS-61-80-017 (1980).

11. J. C. Wyngaard and S. F. Clifford, J. Atmos. Sci., **35**, 1204 (1978).
12. C. A. Friehe, J. C. La Rue, F. H. Champagne, C. H. Gibson, and G. F. Dreyer, J. Opt. Soc. Am. **65**, 1502 (1975).
13. C. W. Fairall, K. L. Davidson, and G. E. Schacher, J. Appl. Meteorol. **18**, 1237 (1979).
14. J. C. Wyngaard, *Workshop on Micrometeorology*, AMS Publication (Science, Ephrata, Pa. 1973), p. 127.
15. C. A. Friehe, Appl. Opt. **16**, 334 (1977).
16. J. C. Wyngaard and P. Lemone, J. Atmos. Sci. **37**, 1573 (1980).
17. J. A. Businger, "Workshop on Micrometeorology," AMS publication (Science Press, Ephrata, Pa., 1973), pp. 76–77.
18. J. A. Businger, J. C. Wyngaard, Y. Izumi, and E. F. Bradley, J. Atmos. Sci. **28**, 181 (1971).
19. J. R. Garratt, Mon. Weather Rev., **105**, 915 (1975).
20. J. Kondo, Boundary Layer Meteorol. **9**, 91 (1975).

Meetings Calendar *continued from page 2888*

1981
October

12–16 Photomicrography course, Chicago *N. Daerr, McCrone Res. Inst., 2508 S. Michigan Ave., Chicago, Ill. 60616*

13–15 6th Ann. Conf. Materials for Coal Conversion & Utilization, NBS, Gaithersburg *S. Schneider, NBS, B-308 Materials Bldg., Wash., D.C. 20234*

19–23 Identification of Small Particles course, Chicago *N. Daerr, McCrone Res. Inst., 2508 S. Michigan Ave., Chicago, Ill. 60616*

19–23 Ceramitec 1982, Munich *W. Marzin, Muenchener Messe-und Austellungsgesselschaft mbH, Messegelaende, Postfach 12 10 09, D-800 Muenchen 12, F.R.G.*

20–23 34th Ann. Gaseous Electronics Conf., Boston *M. J. Boness, Avco Everett Res. Lab., Inc., 2385 Revere Beach Pkwy., Everett, Mass. 02149*

26–28 AIAA Computers in Aerospace 111 Conf., San Diego, Calif. *P. Rye, Tech. Program Chairman, C. S. Draper Lab, P.O. Box 1541, Downey, Calif. 92041*

26–30 **OSA Natl. Mtg.**, Kissimmee, Fla. *Mtgs. Dept., OSA, 1816 Jefferson Pl. N.W., Wash., D.C. 20036*

26–30 Applied Polarized Light Microscopy course, Chicago *N. Daerr, McCrone Res. Inst., 2508 S. Michigan Ave., Chicago, Ill. 60616*

26–30 Laser Safety course, Wash., D.C. *Laser Inst. Am., P.O. Box 9000, Waco, Tex. 76710*

November

? 1st Japanese Fiber Optics & Communications Expo., Tokyo *E. Bond, Info. Gatekeepers, Inc., 167 Corey Rd., Suite 111, Brookline, Mass. 02146*

2–6 APS Div. of Plasma Physics, Wash., D.C. *W.W. Havens, Jr., 335 E. 45 St., N.Y., N.Y. 10071*

3–9 Remote Sensing of Environment Int. Symp., Cairo *Remote Sensing Ctr., ERIM, P.O. Box 8618, Ann Arbor, Mich. 48107*

4–6 2nd EFOC Expo., Koln *Info. Gatekeepers, Inc., 167 Corey Rd., Suite 111, Brookline, Mass. 02146*

9–13 Scanning Electron Microscopy course, Chicago *N. Daerr, McCrone Res. Inst., 2508 S. Michigan Ave., Chicago, Ill. 60616*

9–13 Fusion Methods (Hot Stage) course, Chicago *N. Daerr, McCrone Res. Inst., 2508 S. Michigan Ave., Chicago, Ill. 60616*

9–13 Photographic Science course, Rochester *V. Johnson, RIT-GARC, 1 Lomb Memorial Drive, Rochester, N.Y. 14623*

16–18 Electrophotography, SPSE 4th Int. Conf., Wash., D.C. *R. Wood, SPSE, 7003 Kilworth Lane, Springfield, Va. 22151*

16–18 Reflecting Optics for Synchrotron Radiation Conf., Upton, N.Y. *SPIE, P.O. Box 10, 405 Fieldston Rd., Bellingham, Wash. 98225*

16–20 Laser Fundamentals & Systems course, Chicago *Laser Inst. Am., P.O. Box 9000, Waco, Tex. 76710*

16–20 Microscopical Identification of Asbestos course, Chicago *N. Daerr, McCrone Res. Inst., 2508 S. Michigan Ave., Chicago, Ill. 60616*

16–20 SPIE Integrated Optics and Millimeter and Microwave Integrated Circuits Conf., Huntsville *SPIE, P.O. Box 10, Bellingham, Wash. 98227*

16–20 SPIE Brookhaven Confs. Optics of Short Wavelengths, Upton, N.Y. *SPIE, P.O. Box 10, Bellingham, Wash. 98227*

17–18 13th Ann. Symp. Optical Materials for High Power Lasers, Boulder *H. Bennett, Michelson Lab, Code 38101, Naval Weapons Center, China Lake, Calif. 93555*

18–20 High Resolution Soft X-Ray Optics Conf., Upton, N.Y. *SPIE, P.O. Box 10, 405 Fieldston Rd., Bellingham, Wash. 98225*

23–24 Deformation, Fracture, Wear, and Nondestructive Evaluation of Materials: Physics and Practice Conf., New Orleans *R. Thomson, A113 Materials Bldg., NBS, Wash., D.C. 20234*

23–25 APS Div. of Fluid Dynamics, Monterey, Calif. *W. W. Havens, Jr., 335 E. 45 St., N. Y., N.Y. 10017*

December

9–11 **OSA Optical Fabrication & Testing Workshop, Anaheim** *Mtgs. Dept., OSA, 1816 Jefferson Pl., N.W., Wash., D.C. 20036*

1982

? Remote Sensing of Environment, Int. Symp., Stresa, Italy *J. J. Cook, ERIM, P.O. Box 8618, Ann Arbor, Mich. 48107*

January

6–8 Integrated and Guided-Wave Optics, 6th OSA Top. Mtg., Pacific Grove, Calif. *Mtgs. Dept., OSA, 1816 Jefferson Pl., N.W., Wash., D.C., 20036*

continued on page 2928